Journal of Biomedical Optics

SPIEDigitalLibrary.org/jbo

Real-time temperature determination during retinal photocoagulation on patients

Ralf Brinkmann
Stefan Koinzer
Kerstin Schlott
Lars Ptaszynski
Marco Bever
Alexander Baade
Susanne Luft
Yoko Miura
Johann Roider
Reginald Birngruber

SPIE

Real-time temperature determination during retinal photocoagulation on patients

Ralf Brinkmann,[a,c] Stefan Koinzer,[b] Kerstin Schlott,[a,c] Lars Ptaszynski,[c] Marco Bever,[c] Alexander Baade,[c] Susanne Luft,[a] Yoko Miura,[a] Johann Roider,[b] and Reginald Birngruber[a,c]
[a]University of Lübeck, Institute of Biomedical Optics, Lübeck, Germany
[b]University Hospital of Schleswig-Holstein, Department of Ophthalmology, Campus Kiel, Kiel, Germany
[c]Medical Laser Center Lübeck GmbH, Lübeck, Germany

Abstract. The induced thermal damage in retinal photocoagulation depends on the temperature increase and the time of irradiation. The temperature rise is unknown due to intraocular variations in light transmission, scattering and grade of absorption in the retinal pigment epithelium (RPE) and the choroid. Thus, in clinical practice, often stronger and deeper coagulations are applied than therapeutically needed, which can lead to extended neuroretinal damage and strong pain perception. This work focuses on an optoacoustic (OA) method to determine the temperature rise in real-time during photocoagulation by repetitively exciting thermoelastic pressure transients with nanosecond probe laser pulses, which are simultaneously applied to the treatment radiation. The temperature-dependent pressure amplitudes are non-invasively detected at the cornea with an ultrasonic transducer embedded in the contact lens. During clinical treatment, temperature courses as predicted by heat diffusion theory are observed in most cases. For laser spot diameters of 100 and 300 μm, and irradiation times of 100 and 200 ms, respectively, peak temperatures range between 70°C and 85°C for mild coagulations. The obtained data look very promising for the realization of a feedback-controlled treatment, which automatically generates preselected and reproducible coagulation strengths, unburdens the ophthalmologist from manual laser dosage, and minimizes adverse effects and pain for the patient. [DOI: 10.1117/1.JBO.17.6.061219]

Keywords: temperature; real-time; optoacoustics; photoacoustics; photocoagulation; thermal damage; coagulation; retina; automatic dosage; feedback control.

Paper 11531SSP received Sep. 20, 2011; revised manuscript received Feb. 8, 2012; accepted for publication Mar. 5, 2012; published online May 15, 2012.

1 Introduction

Retinal photocoagulation was introduced in the 1950s by Meyer-Schwickerath, and its application to seal retinal tears has become a clinical standard.[1] By the 1990s, laser photocoagulation has become the standard of care for various indications according to large clinical trials, most prominently the early treatment of diabetic retinopathy study (ETDRS),[2,3] the branch vein occlusion study group,[4] and the collaborative central retinal vein occlusion study.[5]

Recently, photocoagulation has been challenged by intravitreal drug administration, but has remained the gold standard of treatment of peripheral ischemic retinal conditions such as diabetic retinopathy and ischemic vein occlusion.[6] At the macular region, it still represents a first-line or adjunctive therapy in focal diabetic maculopathy[7] and branch vein occlusion. Major advantages of photocoagulation include availability, low cost, and easy handling, making it the therapy of choice even in cases where intravitreal injections may promise minimally better vision. Recent improvements of photocoagulation aim at minimized tissue destruction,[8,9] improved patient comfort,[10] and increased application performance.[11,12] Pilot studies have demonstrated that photocoagulation has not yet been developed up to its best potential.[13–15] This work targets a method which automatically generates uniform lesions by controlling the dosage for every individual photocoagulation spot, with preselectable strength.

For retinal photocoagulation, typically a laser power of 50 to 500 mW is applied for an irradiation time of 20 to 200 ms onto a spot diameter ranging over 50 to 500 μm.[2–4,16–20] It is mainly performed with laser radiation in the green spectral range because of its high absorption at the retinal pigment epithelium (RPE) and choroid. Owing to heat diffusion the adjacent retinal layers are also thermally damaged. The lesions become visible as whitish/grayish lesions under white light visual ophthalmoscopic examination because of increased light scattering after the onset of denaturation. The visibility of the lesions is used as post irradiation dosage control for successful application. In a typical laser lesion irreversible thermal denaturation of the outer and inner retinal segments and the choroid is found.[21]

The therapeutic idea behind photocoagulation depends on the targeted disease. While artificial scar production to prevent retinal detachment is undisputable, the therapeutic effect following panretinal coagulation in diabetic retinopathy is still debatable. The most popular and accepted theory of Wolbarsht and Landers postulates that by denaturation of the photoreceptor cells in the outer periphery the overall oxygen demand, and therefore the neovascularisation in diabetes is reduced. This leads to a stabilized metabolism in the central area which is spared from coagulation;[22] however, the necrosis of the inner neural retina should be avoided in any case.

Address all correspondence to: Ralf Brinkmann, University of Lübeck, Institute of Biomedical Optics and Medical Laser Center Lübeck GmbH, Peter-Monnik-Weg 4, D-23562, Lübeck, Germany. Tel: +49 4515006507; Fax: +49 4515006546; E-mail: brinkmann@bmo.uni-luebeck.de

0091-3286/2012/$25.00

Varying transmission[23] and RPE/choroidal pigmentation[24,25] of a treated eye account for significant effect variations even at a constant laser power. Hence, laser power needs to be permanently observed for ophthalmoscopical whitening and must be adjusted accordingly. Ophthalmoscopically visible whitening of a lesion takes up to a whole day to fully develop. During a treatment session of several hundred lesions, it is thus not feasible to wait long enough to finally judge every single lesion. Long exposure times of 200 ms grant a wide therapeutical window, but poor axial confinement of a lesion, and the undesired coagulation of the inner retinal layers is likely.[26] In order to reduce the thermal damage caused by heat diffusion, newer approaches reduce the irradiation time down to 10 ms;[26] however, this approach increases the risk of choroidal rupture and bleeding because fast heat deposition can lead to disruption if the vaporization temperature is exceeded. Thus, the effective therapeutic window, which is defined as the ratio of threshold power for rupture to the threshold power for coagulation, decreases.[26,27] Nevertheless, this approach has already led to reduced pain for the patient, and a reduced treatment time in combination with patterned coagulation.[28] In summary, slow occurrence of whitening and the conflicting needs to spare the neuroretina while retaining a wide therapeutic window all result in unavoidable lesion inhomogeneity as well as over- and under-effects of conventional photocoagulation dosage.[29] In the worst case, full thickness retinal coagulation causes extended scotoma. Retinal ruptures and choroidal bleedings lead to extensive, unnecessary tissue destruction with a risk of secondary choroidal neovascular membrane formation. This problem has for a long time been recognized[30] and first attempts to control the photocoagulation strength by regulating the power of the treatment laser by the onset of light scattering were investigated in the 1980s.[31]

The extent of coagulation depends on the temperature increase and the time of temperature elevation during the irradiation period. It can be described by the thermal damage theory of Arrhenius.[32] The temperature rise finally depends on the amount of absorbed light; thus, it not only depends on the laser settings, but also on the retinal/choroidal pigmentation, which can vary by up to a factor of four in humans.[33] Further, the amount of light scattering within the eye globe is unknown, and mainly depends on the patient's lens condition, which cannot be individually quantified.[23] In case of a treatment time exceeding several seconds, as in transpupillary thermal therapy (TTT), the cooling effect of the perfusion has to be taken into account as well.[34]

In this project, an optoacoustic (OA) method is used to determine the temperature rise during photocoagulation, with the ultimate goal to control the coagulation process by the temperature course. The ability to measure temperature changes by optoacoustics has first been described for soft tissue heating *in vitro*,[35] and in patients' eyes during selective laser therapy of the retina.[36] This technique was further improved and quantified in the following years.[34,37–39] The temperature threshold required to thermally damage the RPE in the time range of 0.1 to 1 sec was recently determined by Denton et al. to $53 \pm 2°\mathrm{C}$.[40] It can be assumed that the required temperature to damage the adjacent photoreceptors is similar. However, because the photoreceptors only absorb a few percent of the incident light, heat diffusion from the RPE is required to achieve these temperatures. Consequently, the RPE needs to be heated higher. The technique for real-time optoacoustic temperature measurements was investigated on tissue samples for thermal therapy[21,22] as well as fundus tissue for TTT. For the latter, a typical irradiation time of one minute on large spot diameters of 2 to 3 mm was used, and the capability and accuracy of this approach was demonstrated on rabbits; however, it has not been proven in clinic trials yet.[34] In order to use this method for photocoagulation with its much shorter irradiation times and smaller spot diameters, the TTT-setup needed to be modified. In this paper, the background and technique of OA temperature monitoring will briefly be reviewed, and the very first measurements on patients will be presented and discussed.

2 Optoacoustic Pressure Generation

If a collimated laser beam with a top hat beam profile and a pulse duration τ_p smaller than the thermal confinement time (negligible heat diffusion) is applied onto a homogeneous absorber with the absorption coefficient μ_a and negligible light scattering, the energy density $E(z)$ is induced within the absorber. $E(z)$ is proportional to the absorption coefficient μ_a and the radiant exposure H, and decreases exponentially according to Beer's law of absorption in the axial z-direction:

$$E(z) = \mu_a \cdot H \cdot e^{-\mu_a \cdot z}. \tag{1}$$

The absorbed energy leads to a temperature increase $\Delta T(\vec{r}, t)$, which can be described with the heat diffusion equation containing ρ as the density, κ as the thermal diffusivity, and C_p as the heat capacity at constant pressure of the absorber. For limited cases, the equation can be solved analytically with a model described in detail by Birngruber:[32]

$$\frac{\partial \Delta T(\vec{r}, t)}{\partial t} - \kappa \cdot \nabla^2 \Delta T(\vec{r}, t) = \frac{E(z)}{\tau_p \cdot \rho \cdot C_p}. \tag{2}$$

For times shorter than the thermal confinement time, Eq. (2) can be integrated, and an instantaneous temperature rise $\Delta T(z)$ is obtained according to:

$$\Delta T(z) = \frac{1}{\rho \cdot C_p} \cdot E(z). \tag{3}$$

If the pulse duration further fulfils the conditions of acoustic confinement (no pressure balance during heating), the temperature rise leads to a pressure increase inside the absorber because in most materials the density decreases with temperature.[41]

$$P(z) \sim \Gamma(T) \cdot E(z) \qquad \Gamma(T) = \frac{\beta(T) \cdot c_s(T)^2}{C_p(T)}$$
$$\text{with } \beta(T) = \frac{1}{\rho}\frac{\partial \rho}{\partial T}. \tag{4}$$

The pressure rise $P(z)$ is proportional to the energy density $E(z)$ and the temperature-dependent, dimensionless Grüneisen parameter $\Gamma(T)$, which contains the thermal expansion coefficient β, the speed of sound c_s and the heat capacity C_p. If the laser pulse duration τ_p is longer than the acoustic transit time but shorter than the thermal relaxation time, an average pressure $\bar{P}$ is obtained inside the absorber, which depends on the ratio of pulse duration τ_p to acoustic transit time τ_{ac}.[42]

$$\bar{P} \sim \Gamma(T) \cdot E_{\text{abs}} \cdot \left(\frac{1-e^{-\tau}}{\tau}\right) \quad \tau = \frac{\tau_p}{\tau_{\text{ac}}} \quad E_{\text{abs}} = A \int E(z)\text{d}z. \tag{5}$$

The pressure increase leads to an expansion of the absorbing volume proportional to $\Gamma(T)$ and the absorbed pulse energy E_{abs} over the beam area A. As a consequence, a thermoelastic, bipolar pressure wave is generated. The pressure wave emission and propagation can be described by the photoelastic wave equation with Ψ as the velocity potential, and $\Delta E(\vec{r},t)$ the energy density:[41]

$$\Delta\Psi - \frac{1}{c_s^2}\frac{\partial^2\Psi}{\partial t^2} = \frac{\Gamma}{\rho c_s^2}\frac{dE(\vec{r},t)}{dt} \qquad p(t) = -\rho\frac{\partial\Psi}{\partial t}. \tag{6}$$

The solution of Eq. (6) is an emerging pressure wave that varies in amplitude and phase over the regarded volume in front of the target. The wave depends on the shape and volume of the absorber.

In case of retinal irradiation, the pressure wave needs to propagate through the eye globe before it can be detected at the cornea. The wave amplitude is attenuated during propagation through the eye by absorption, and acoustic impedance mismatches at the lens, iris, and cornea. Its frequency spectrum is also altered owing to the increasing water absorption for frequencies higher than about 10 MHz. Finally upon detection, the shape, dimensions, material, sensitivity, frequency response, and amplification of the transducer influences the conversion of acoustic to electric energy. However, for every individual source at the retina, the detected peak pressure amplitude p_{max} is proportional to the product of $\Gamma(T) \cdot E_{\text{abs}}$:

$$p_{\text{max}}(T, E_{\text{abs}}) \sim \Gamma(T) \cdot E_{\text{abs}}. \tag{7}$$

3 Non-Invasive Real-Time Temperature Determination

3.1 *Background*

In order to determine the temperature of tissues, one can make use of the temperature dependence of $\Gamma(T)$. For water as the main component of soft tissue the temperature dependencies of c_s and C_p are negligible compared to that of β according to Eq. (4). Between 37°C and 50°C, β increases by 26.46%, whereas c_s and C_p increase only by 1.24% and 0.05%, respectively.[34] In the range of 10°C to 100°C, the Grüneisen parameter can be approximated by a 2nd order polynomial:[43]

$$\Gamma(T) \sim [(T^2 - T_0^2) - 2T_{\text{max}}(T - T_0)]. \tag{8}$$

$T = T_0$ indicates the temperature for which $\Gamma(T) = 0$ and $\Gamma(T)$ reaches its maximum for $T = T_{\text{max}}$. For water $T_0 = 3.98$ °C at its state of maximal density. If Eqs. (7) and (8) are combined, and T_0, T_{max}, and the product $S \cdot E_{\text{abs}}$ are known, then the optoacoustically determined temperature $T_{\text{OA}}(t)$ can be derived from the measured pressure amplitude $p_{\text{max}}(t)$ to:

$$T_{\text{OA}}(t) = T(p_{\text{max}}, t) = T_{\text{max}} - \sqrt{(T_{\text{max}} - T_0)^2 + \frac{p_{\text{max}}(t)}{S \cdot E_{\text{abs}}}}. \tag{9}$$

If the tissue is heated uniformly, $T_{\text{OA}}(t)$ directly corresponds to the tissue temperature. S is the proportionality constant accounting for Grüneisen proportionality and all attenuations for the propagating wave as discussed above. The product $S \cdot E_{\text{abs}}$ is at first unknown and varies for every single location at the retina.

3.2 *Retinal Tissue Characterization*

In order to determine the tissue-specific parameters, T_{max} and T_0 for retinal tissue, the pressure amplitudes and corresponding temperatures were measured simultaneously on freshly enucleated porcine eyes as shown in Fig. 1.

The eyes were fixed in a special holder which allowed laser heating from rear. A cw diode laser (LISA laser OHG) with a maximum power of 90 W at 940 nm was used for fast tissue heating. The IR-beam was expanded to a top hat diameter of 18 mm to achieve a uniform temperature rise at the central retinal region. Furthermore, thin thermocouples (Newport Electronics GmbH, HYP0-33-1-T-G-60-SMPW-M, tip diameter 200 μm) were pierced in the eye globe close to the center of acoustic probing in order to measure the actual fundus temperature. During heating with a temperature rise time of about 100 °C/ min, probe laser pulses (CrystaLaser Inc., QG-523-1000: 523 nm, 3.5 μJ, 75 ns, 1 kHz) were applied with a top hat beam diameter of about 100 μm. Pressure transients were measured with an annular piezo ceramic transducer (PZT) with high sensitivity in the MHz frequency range (Medical Laser Center Lübeck GmbH), which was embedded in a contact lens (Mainster OMRA-S Focal/Grid) to be used to apply the laser beam into the eye. The transients were electrically amplified and processed with LabVIEW to calculate the temperature rise from the measured pressure amplitudes. Figure 2 shows the measured increase of the pressure amplitudes in dependence of the specimen temperature. The dashed lines in Fig. 2 are exemplary second order polynomial fits to individual heating curves, the solid line is the fit received by averaging over all single fits. The fits are extrapolated beyond the data range to determine the tissue-specific parameters, T_0 and T_{max}. T_0 and T_{max} cannot be measured directly, because the tissue would undergo phase

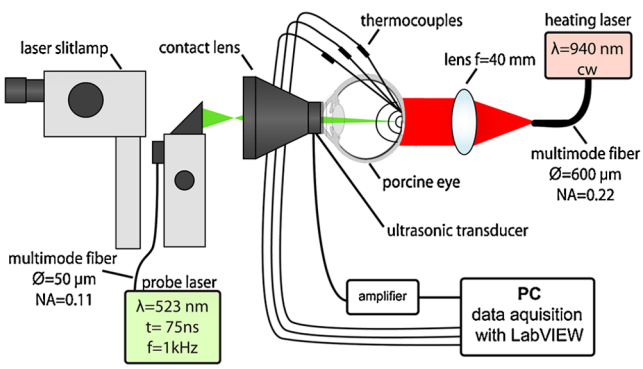

Fig. 1 Setup to determine the characteristic retinal tissue parameters T_0 and T_{max}. Enucleated porcine globes were heated from rear with a cw diode laser while the temperature at the retina was measured with thermocouples. Simultaneously, acoustic pressure transients were excited with nanosecond probe laser pulses. The pressure transients were detected with an ultrasonic pressure sensor integrated in the contact lens.

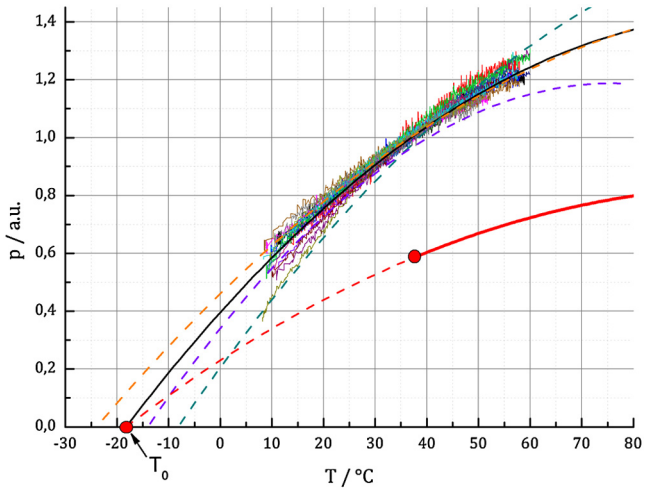

Fig. 2 Measured pressure amplitudes p_{max} over probe temperature determined by thermocouples. The data points are fitted with a second order polynomial (dashed curves: exemplarily individual fits, solid black curve: average over all specimens). Lower red curve: strategy to determine temperatures in a clinical setting (explanation within the text).

transitions at $T = 0$ and above the onset temperature for coagulation, which would change the physical parameter associated with $\Gamma(T)$ according to Eq. (4).

Figure 2 shows a significant pressure increase of 125% from 10°C to 60°C, and 25% from 37°C to 60°C. With a least square regression fit, T_0 and T_{max} were determined to be $T_0 = -17.0 \pm 5.0\,°C$, and $T_{max} = 93.3 \pm 15.6\,°C$ as an average value with standard deviation of the parameters obtained from 18 porcine eyes.

3.3 *Temperature Determination During Retinal Photocoagulation*

When probing optoacoustically, the product $S \cdot E_{abs}$ in Eq. (9) is at first unknown. To overcome this problem, probe laser pulses are applied just before the treatment laser begins. In this case, an arbitrary pressure amplitude p_{max} is measured (e.g., $p_{max} = 0.6$ in Fig. 2, red dot), which corresponds to the body temperature of $T(p_{max}) = 37\,°C$. Thus, solving Eq. (9) for $S \cdot E_{abs}$, this product is unequivocally determined for the individual spot. When the treatment laser begins after this pressure/temperature calibration, the temperature can be unambiguously deduced from the increasing pressure amplitudes using Eq. (9) (which is also graphically depicted, shown in the red curve in Fig. 2), as far as the coupling constant S and the tissue-specific parameters T_0 and T_{max} do not change. Fluctuations in the probe pulse energy sequence can proportionally be compensated, which can be used to improve the signal to noise ratio.

3.4 *Average Temperature Rise in the Probed Volume and RPE Peak Temperature*

During photocoagulation, probe and treatment radiation are applied through the same fiber, and the temperature is probed over the whole irradiated volume. This process needs to be addressed with respect to temperature monitoring. During tissue heating, a transiently changing spatio-temporal temperature profile builds up at the treatment location. To quantify the temperature evolution, Eq. (2) was solved with the thermal parameters of

Table 1 Model parameters for the human fundus as used for the temperature calculations.

	Thickness [μm]	μa [1/cm]	Absorption [%]
RPE	6	1204	51
Bruch's membrane	4	0	0
Pigmented choroid	400	270	49

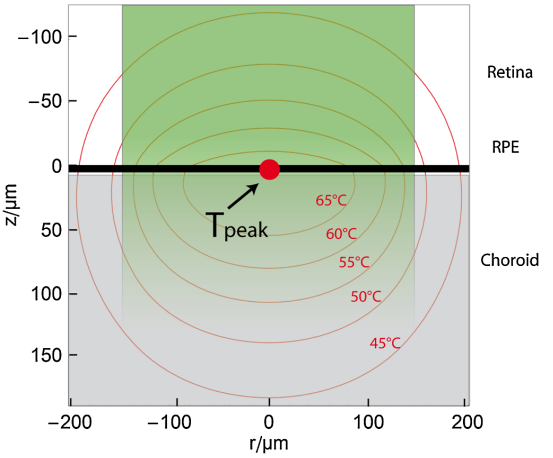

Fig. 3 Calculations for different isotherms in the cross section of the chorioretinal junction after an irradiation of 100 ms for a laser power of 40 mW applied onto a spot diameter of 300 μm. The green color demarks the irradiated volume and the fading green indicates the light absorption towards choroidal depth. The temperature in this volume is probed. The red dot denotes the point of highest temperature T_{peak}, which is in the center of the spot inside the RPE.

water. The characteristic parameters of human fundus absorption are shown in Table 1, and were taken from Hammer et al.[44] These data fit quite well to the few human data available in the literature, e.g. from Gabel et al.[24] Selected solutions for a spot diameter of 300 μm and a laser power of 40 mW applied to the retina are shown in a cross section in Fig. 3, and for $\Delta T(t)$ and over r, z and t in Fig. 4. During the onset of irradiation within the first 100 μs, the temperature profile follows the absorption characteristics, which is modified by heat diffusion thereafter. The temperatures scale linearly with laser power for all locations and times. An equilibrium temperature profile is reached within a time frame of about 1 s, depending on the spot size and absorption profile.

The peak temperature $T_{peak}(t)$ is always achieved in the center of the spot at the level of the RPE. Often this peak temperature is of interest, because here the coagulation is expected to start. In this case, it can be regarded as a threshold temperature for thermal denaturation in case of just barely visible lesions. Since optoacoustics in this approach reveals the average temperature over the whole probed volume, a conversion from this average to the peak temperature is necessary. This can be treated mathematically. Therefore, at first the mean temperature across each depth layer $T_{mean}(t, z)$ for a certain beam radius R is calculated:

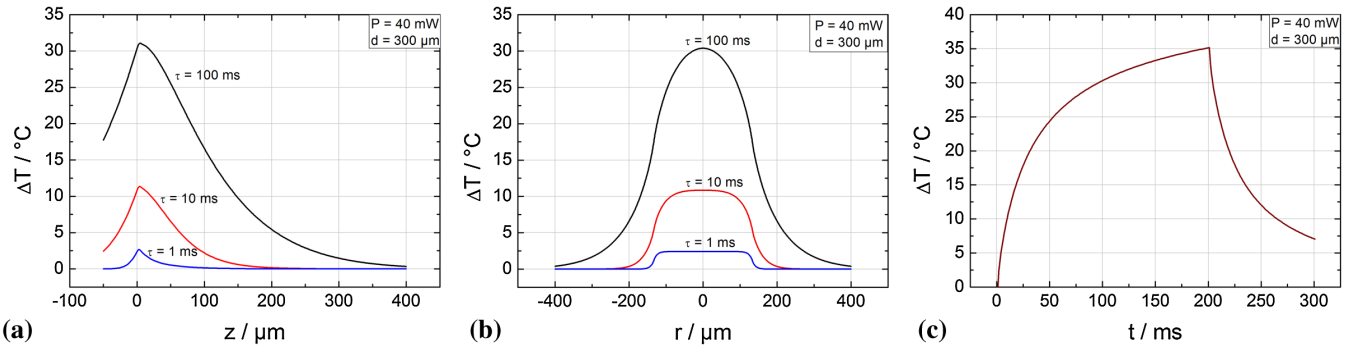

Fig. 4 Calculated temperature profiles using a laser power of 40 mW onto a spot diameter of 300 μm. (a) Axial temperature profile (negative values: retina, zero: RPE surface, positive values: choroid) for times of 1,10 and 100 ms after the onset of heating. (b) Lateral temperature profile for times of 1,10 and 100 ms after the onset of heating. (c) Temporal temperature rise $\Delta T_{\mathrm{peak}}(t)$ at the center of the RPE.

$$T_{\mathrm{mean}}(t,z) = \frac{1}{A} \cdot \int_0^{2\pi} \mathrm{d}\phi \cdot \int_0^R T(t,r,z) \cdot r \cdot \mathrm{d}r = \frac{2}{R^2} \int_0^R r \cdot T(t,r,z) \cdot \mathrm{d}r. \quad (10)$$

If we consider that the probe beam is exponentially attenuated towards penetration depth according to Eq. (1) and as sketched in Fig. 3, then the average probed temperature in the irradiated volume $T_{\mathrm{volume}}(t)$ must also be weighted exponentially:

$$T_{\mathrm{volume}}(t) = \mu_a \int_0^{\infty} T_{\mathrm{mean}}(t,z) \cdot e^{-z\cdot\mu_a} \cdot \mathrm{d}z. \quad (11)$$

The average weighted temperature $T_{\mathrm{volume}}(t)$, which is probed, depends on the time and the absorption, and is equal to the optoacoustically determined temperature: $T_{\mathrm{OA}}(t) = T_{\mathrm{volume}}(t)$. The relation between the peak temperature $T_{\mathrm{peak}}(t)$ in the center of the spot at the RPE ($r = 0$, $z = 0$) and $T_{\mathrm{OA}}(t)$ is given by the time-dependent conversion function $f(t)$:

$$f(t) = \frac{T_{\mathrm{peak}}(r = z = 0, t)}{T_{\mathrm{OA}}(t)}. \quad (12)$$

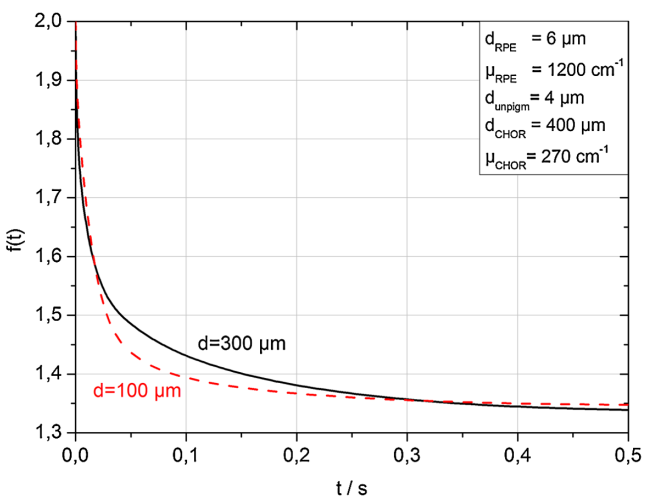

Fig. 5 Calculated conversion functions $f(t)$ as the ratio of the peak temperature in the center of the RPE, $T_{\mathrm{peak}}(t)$, and the mean weighted temperature of the probed volume $T_{\mathrm{volume}}(t)$, which is equal to the optoacoustically obtained temperature $T_{\mathrm{OA}}(t)$. Calculations for laser spot diameters of 100 and 300 μm are shown.

Figure 5 shows $f(t)$ for two different radii (50 and 150 μm). As long as the radiation is completely absorbed within the RPE and choroid, and the absorption ratio between RPE and choroid keeps constant, $f(t)$ does not depend on the absorption coefficient and the laser power. This is important for the applicability and reliability of optoacoustic temperature determination because absorption varies inter- and intra-individually for each laser spot.

4 Clinical Study and First Clinical Results

The study comprised 20 patients with a clinical indication for panretinal and sometimes central photocoagulation. The study was conducted to determine the retinal temperature rise during photocoagulation. Diseases to treat included diabetic retinopathy, retinal vein occlusion, and occlusive retinal vasculitis. Each patient's body temperature was measured before the laser treatment. Irradiation was performed with defined laser settings inside (100 μm, 100 ms, gentle whitening) or outside the arcades (100 or 300 μm, 20 to 200 ms, power titration around threshold power) of the fundus. Twenty to 40 study lesions were applied and evaluated by fundus photography and OCT (Heidelberg Engineering, Spectralis) after 1 h, and at different times thereafter. Afterwards, the treatment was continued according to clinical routine requirements. All data were processed and evaluated after the treatment was completed. The clinicians had no access to the recorded OA data during treatment. The study had been reviewed and approved by the institutional ethics committee.

A modified photocoagulation laser (Carl Zeiss Meditec AG, Visulas 532 s, $\lambda = 532$ nm) was used for treatment. The treatment radiation is superimposed by ns-probe laser pulses applied with a repetition rate of 1 kHz and adjustable pulse energies (4 to 12 μJ). The radiation is transmitted via a 50-μm core diameter fiber (Carl Zeiss Meditec AG, NA = 0.11) through a laser slit lamp (Carl Zeiss Meditec AG, SL 130). An equal contact lens and comparable data processing was performed as described in Sec. 3.2.

Prior to each treatment exposure, 20 calibration laser pulses were applied in order to determine the product $S \cdot E_p$ according to Eq. (9). Figures 6 and 7 show exemplary fundus photos of two patients, treated with a 300 or 100 μm laser spot diameter. For selected spots, the peak temperature profiles are plotted in Figs. 6 and 7, and OCT images are shown exemplary. The peak temperature was calculated according to Eq. (12): $T_{\mathrm{peak}}(t) = f(t) \cdot T_{\mathrm{OA}}(t)$ using $f(t)$, T_0, and T_{max} as described above.

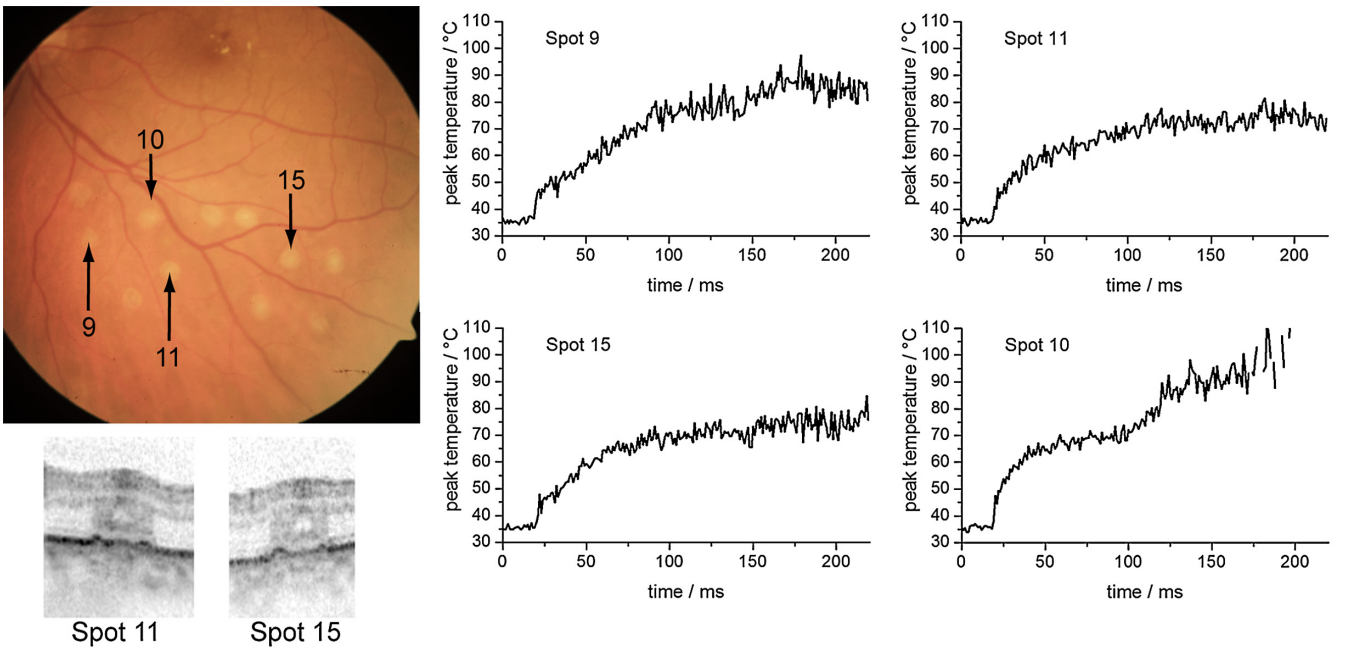

Fig. 6 Fundus picture, selected peak temperature curves and OCT images (1 h after irradiation) of patient No. 4. Retinal laser spot diameter: 300 μm, cw laser power: 200 mW, treatment irradiation time: 200 ms, probe pulse energy: 12 μJ.

Figure 6 shows the temperature profiles for 300 μm spot diameter using a treatment power of 200 mW and a probe pulse energy of 12 μJ. The plots show 20 calibration pulses (first 20 ms) which were normalized to body temperature as described above. No temperature rise is observed here, since the calculated radiant exposure for a probe pulse is only $H = 17$ mJ/cm^2, which corresponds to a very short and only transient temperature rise of 4.9°C according to Eq. (2). Because only about 30% of the light reaches the target site (see below), the transient temperature peak is most likely only about 1.5°C. Overall, the probe pulses account for an average power of 12 mW, thus 6% of the treatment power, which is their contribution to the retinal heating. After 20 ms, the treatment laser starts and the temperature rises quickly until the treatment beam is ceased after 200 ms. It is evident from the plots that the temperatures increase almost as predicted by heat diffusion calculations depicted in Fig. 4. The maximal peak temperatures after 200 ms are found around 70°C to 85°C at the end of the irradiation period for weak coagulations, while in stronger ones they can exceed 100°C. Spot no. 10 shows a second temperature rise after around 100 ms. This is most likely caused by a slight eye movement (see fundus picture with a slightly elongated

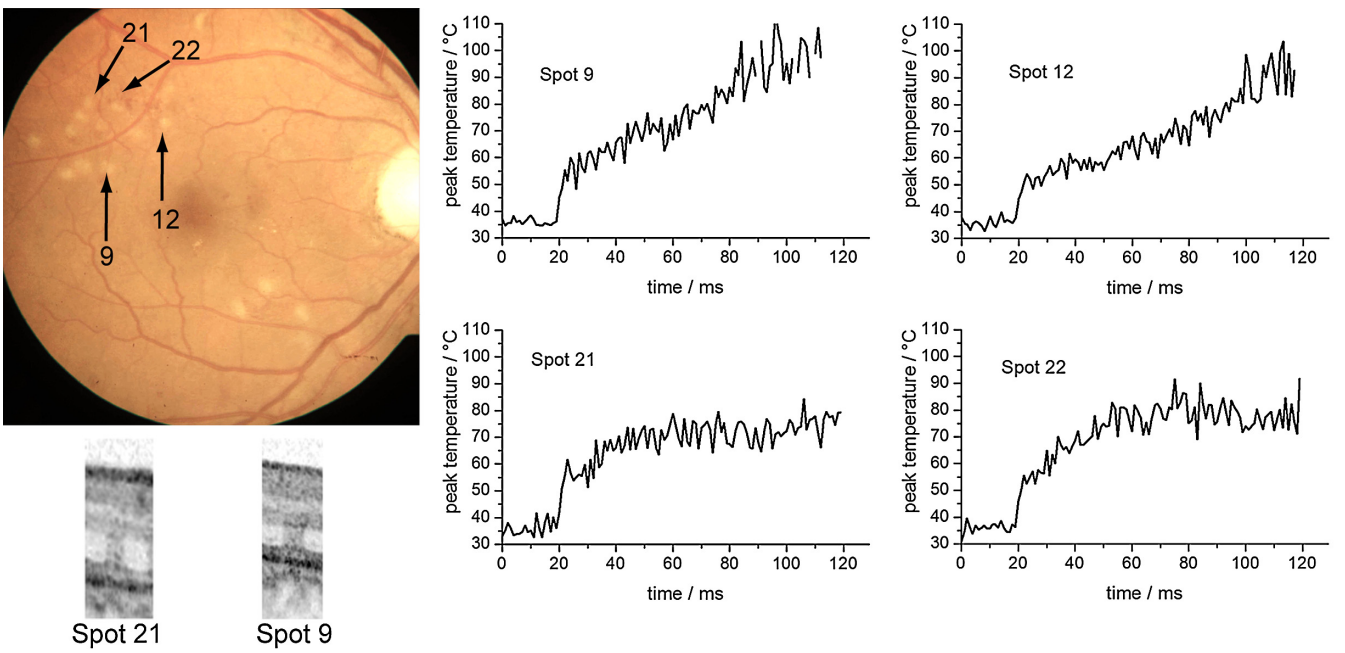

Fig. 7 Fundus picture, selected peak temperature curves and OCT images (1 h after irradiation) of patient No. 1. Retinal laser spot diameter: 100 μm, laser power: 70 mW, treatment irradiation time: 100 ms, probe pulse energy: 4 μJ.

coagulation spot). Figure 6 also shows exemplary OCT pictures of spot Nos. 11 and 15. Both pictures indicate that inner and outer retinal layers are affected.

Figure 7 shows exemplary data of a patient treated with a 100 μm spot diameter and an irradiation time of 100 ms. The signal-to-noise ratio is worse than the 300 μm spot applications, since the probe pulse energy was reduced to 4 μJ. Generally, comparable temperatures and temperature profiles for 100 and 300 μm spot are achieved; however, with around 3 times less laser power for the 100 μm spot. This is in good agreement with heat diffusion theory, which predicts almost the same temperature rise when increasing the laser power proportionally with the spot diameter. OCT pictures for two spots demonstrate that the photoreceptor layers are coagulated. The lateral extent of the damage seems to be larger for spot No. 9, which corresponds to a higher peak temperature of around 100°C at the end of the heating period. This spot was identified with a notable eye movement. Further, some more spots were found with a temperature curve not strictly following the expected slope according to the heat diffusion theory, e.g., the linear increase of spot Nos. 9 and 12. This can most likely be attributed to slight eye movements or saccades.

5 Discussion

A clinical study was conducted to investigate optoacoustic temperature measurements during laser photocoagulation at the retina. The generated pressure transients were processed to determine the average temperature rise during heating and coagulation, and were further evaluated to reveal the peak temperature at the RPE over time.

5.1 *Acoustic Pressure Detection and Temperature Determination*

First of all, it could be demonstrated that ns laser pulses with pulse energies in the lower μJ range are sufficient to induce thermoelastic acoustic transients that are strong enough to be detected with an ultrasonic transducer embedded in a modified clinical contact lens with a sufficient signal-to-noise ratio. However, all features of the transducer, like dimensions and frequency response, are not relevant for the principle of function, as long as the transducer is at least sensitive enough to detect the pressure waves with sufficient signal/noise, and as long as the transducer operates in the linear regime, which is both the case here. Mathematical simulation and Fourier transformation with the equations given show a broad frequency emission spectrum with a peak at 6.6 MHz, and broad spectrum from less than 1 to more than 20 MHz, thus a significant overlap with the transducer's spectral range. The transducer is so far not optimized with respect to maximal performance, which is under current development. Furthermore the distance from transducer to retina varies from patient to patient, it even varies within a patient's eye, depending on the treatment location with respect to the eye's optical axis. The measured amplitudes vary strongly from site to site due to the focusing characteristics of the transducer; however, this all cancels out because for each spot, the pressure amplitude is calibrated to body temperature just before the coagulation starts.

Further, a method is presented how the pressure amplitude from the whole target volume can be transferred to the retinal temperature rise and the peak temperature at the RPE. Due to exponential attenuation of the probe beam by absorption over depth, pressure contribution from deeper layers becomes exponentially less and less. Thus, the pressure is weighted exponentially with the depth in the choroid (Fig. 3), which leads to an averaged and weighted pressure response.

During heating the pressure contribution from each voxel in this volume depends on its temperature. Figure 4 shows that the temperature/pressure relationship is almost linear between 37°C and 60°C. With this assumption, the averaged, weighted pressure increase is proportional to the averaged, weighted temperature increase within the cylindric volume which is probed. The heat diffusion equation is used to calculate the peak temperature increase at the center of the RPE (as a function of time), and the average weighted temperature increase over time in the cylindrical volume probed by the pulsed laser. The ratio is referred to as $f(t)$. By combining the calculated temperature from heat diffusion theory and that gained from pressure amplitude experimentally, we get the unknown but wanted peak pressure amplitude increase with the measured averaged and weighted pressure $p(t)$ by simple proportionality. Finally, we can calculate the wanted peak RPE temperature $T_{\mathrm{peak}}(t)$ by means of Eqs. (9) and (12).

5.2 *Clinical Temperatures for Photocoagulation*

The clinical data evaluation shows similar temperature profiles and absolute temperatures for most of the lesions ranging from 70°C to 100°C. The observed temperature slopes are within the range which is expected from heat diffusion theory. Also, a number of applications showing significantly different slopes were observed. Most of these spots show slight elongations in their fundus appearance, thus eye motion due to slight eye or contact lens movements or saccades can be assumed. In these cases, the individual calibrations according to Eqs. (7) and (9) are lost, and the calculated temperatures are inaccurate (see discussion on principal limitations below). The data suggest that sensitivity to eye movements is more pronounced for smaller spot diameters, which is validated here.

Furthermore, it is interesting to compare the temperatures with those predicted by the standard Arrhenius theory for the threshold of coagulation. The most commonly used parameters for retinal coagulation according to Vassiliadis and Birngruber[32,45] predict a temperature threshold of 75°C for a 100-ms coagulation, and slightly lower for a 300-ms coagulation. We found lower coagulation threshold temperatures in this study. This topic is discussed in more detail in the literature by Schlott et al.[46]

Additionally, the achieved temperatures, calculated on the one hand and measured on the other, require a three- to four-times higher laser power in the clinical setting compared to the calculation with the commonly used human model parameters. Figure 6 shows a peak temperature rise of 40°C (spot Nos. 11 and 15) and 50°C (spot no. 9) using a laser irradiation with a power of 200 mW, while calculations (Fig. 4) reveal $\Delta T = 35\,^{\circ}\mathrm{C}$ after 200 ms for a laser power of 40 mW. This refers to 46 and 57 mW for $\Delta T = 40\,^{\circ}\mathrm{C}$ and 50°C, respectively. Thus roughly only 20% to 30% of the laser light reaches the target spot size at the 70% to 80% of light is reflected and scattered on its way through the contact lens and human eye globe. This is in accordance with the data published by Boettner and Wolter,[23] who measured the direct light transmission through the whole eye and found a strong decrease with age. Scattering within the eye can be as high as 70% even with the small number of human eyes they had available. Additionally, pathological retinal conditions such as edema or exsudates might have an influence

on light scattering and the biological tissue response. It is to be expected that edematous retina requires higher laser power to achieve a given temperature rise. OCT provides information about the morphological damage extent. Detailed studies concerning the relation between measured temperature and OCT findings of the lesions are under investigation.

5.3 *Temperature Determination: Limitations*

Even though first clinical data could be obtained in humans, the OA method to monitor temperatures has some limitations and points which need to be addressed. The tissue-specific Grüneisen parameter $\Gamma(T)$ describing the thermoelastic expansion is unknown for human retinal tissue. As a substitute, experiments on enucleated porcine eyes as well as on excised porcine and rabbit fundus tissue[34] were performed. Large specimens were heated systemically by laser water cuvette or by using hole eye globes as shown here to induce spatially homogeneous temperatures at the fundus, and determine OA temperature/pressure relations for different probe laser parameters. Evidently, all results on the temperature/pressure relationship show the same parabolic dependence.

The accuracy of temperature determination with respect to the specific tissue parameter T_0 and $T_{\max}$ can be estimated: $T_0 = -17.0 \pm 5.0\,°\mathrm{C}$ and $T_{\max} = 93.3 \pm 15.6\,°\mathrm{C}$ were determined as average values. When the standard deviations are used, e.g., $T_0 = -22\,°\mathrm{C}$ and $T_{\max} = 108.9\,°\mathrm{C}$, resulting in a flatter calibration curve, or $T_0 = -12\,°\mathrm{C}$ and $T_{\max} = 77.7\,°\mathrm{C}$ as a steeper curve, then the errors for temperature calculation during measurements are maximal $\pm 2.2\,°\mathrm{C}$ in the clinically relevant regime of temperatures.[47]

Moreover, it is uncertain how these tissue parameters of young and healthy animal eyes can be transferred to older and pathologically altered human eyes. However, no strong deviations are expected because it is very unlikely that the thermal expansion coefficient β, the speed of sound c_s, and the heat capacity of the tissue C_p according to Eq. (4) vary strongly. Regardless, this fact has to be kept in mind as a potential source of mismatch, e.g. by slight eye movements during irradiation, which alters the whole calibration. The different absorptions do not play a role with respect to their energy absorption, because they are normalized.

5.4 *Considerations on the Maximum Temperature at the RPE*

When using the same application setup for probing and heating of tissue as done here, optoacoustics determines the mean temperature of all irradiated absorbers, mainly the melanin granules, weighted with an exponential axial decrease. The ratio between the peak temperature in the center of the beam at the RPE, which often is of most interest, and the average temperature in the target volume can be retrieved mathematically. The central peak and mean weighed temperature according to Fig. 4 were compared to experimental results, and deviation of less than 7% was found.[47] The conversion function $f(t)$ changes over time since the lateral temperature profile develops from a top hat to a more Gaussian distribution due to heat diffusion. Since the heat dissipation is different for different spot diameters, $f(t)$ also depends on the absorber dimensions. The conversion function, however, does not depend on the absorption coefficient for a single homogeneously pigmented layer. If more than one absorbing layer is involved, and the ratio of their absorption coefficients varies, $f(t)$ slightly varies, too. Details on this potential source of error for different RPE/choroidal absorption ratios are given in the literature.[48] Phase-sensitive optical coherence tomography (OCT) allows the determination of retinal tissue expansion, and thus temperature evolution during photocoagulation in four-dimensions (4-D) with very high resolution in the μm range. It can be used to analyse the accuracy of temperature monitoring for this optoacoustic method in detail.[49] On top of this, the denaturation process and the associated volume change can be observed with OCT and be separated from thermoelastic expansion.

For irradiations far exceeding the coagulation threshold, reliable OA-temperature readings cannot be expected. Due to tissue denaturation, the Grüneisen-parameter changes, and the temperature/pressure calibration becomes invalid. Further, increased light scattering combined with a changing absorption profile leads to modification of spatial heating.[50] Also some energy is required for the protein phase transition during denaturation.

Motional artifacts related to the hand-held contact lens and patient's eye movements and saccades might account for another source of error. In general, slight movements of the laser spot during irradiation might change the calibration settings, and transiently cease the temperature increase. Thus, temperature readout in these cases is inaccurate from the time of movement, as could be exemplary observed for spots Nos. 9, 10, and 12 in Figs. 6 and 7. Thus, the displayed temperatures should be analyzed and interpreted with care, and with regard to the discussed effects. Further investigations are needed to clarify this in more detail.

6 Conclusion

It has been shown that optoacoustics can serve to measure increasing pressure amplitudes during retinal photocoagulation, which can be used to calculate the temperature during the irradiation process; however, the method has some limitations as discussed above. In this ongoing project it has been shown *ex vivo* on enucleated porcine eyes,[50] and *in vivo* on rabbit eyes[46,51] that these data can be processed in real-time in order to automatically control the extent of laser lesions. Over a wide range of laser powers, equally sized lesion diameters could be obtained in porcine eyes *ex vivo*, as well as in rabbit eyes *in vivo* by a real-time automatic laser switch-off algorithm when the appropriate temperature is reached for a certain time.[46,51,52] The first clinical data with automatic feedback controlled photocoagulations are expected in 2012.

In conclusion, all the data look very promising to successfully realize such an automatic dosage control for generating a pre-selected coagulation strength. A temperature-feedback control would also allow to apply sub-threshold laser lesions with a well-defined temperature rise in order to stimulate the neural retina without any irreversible thermal damage.

Scientifically, this method can be used to reiterate the Arrhenius parameters or thermal denaturation of retina.[46] The results of numerous clinical trials on the efficacy of photocoagulation can significantly be improved when similar coagulation strengths and depths are induced in all treatment sites. Moreover, short term coagulations with 20-ms pulse duration, which have become common since the introduction of patterned laser coagulation, strongly reduce the pain for patients.[10] An automatic dosage control system would merge the advantages of reduced pain due to shallow coagulations with a high safety

level like in standard 200-ms exposures. Automatic dosage control can also be applied for 20-ms exposures by a fast temperature-related power control. This is particularly useful in pattern coagulation devices like PASCAL (Optimedica/TopCon) or VISULAS VITE (Carl Zeiss Meditec).

Acknowledgments

This collaborative project is supported by the German Ministry of Research and Technology (BMBF) under the Innovation Price for Advancing Medical Technology 2006, Grant No. 01EZ0732 (Medical Laser Center Lübeck), No. 01EZ0733 (Institute of Biomedical Optics), No. 01EZ0734 (Department of Ophthalmology, University Hospital of Schleswig-Holstein, Campus Kiel), and No. 01EZ0735 (Carl Zeiss Meditec AG).

References

1. G. Meyer-Schwickerath, "Light coagulation: a method for treatment and prevention of the retinal detachment," *Graefes Arch. Ophthalmol.* **156**(1), 2–34 (1954).
2. Early Treatment Diabetic Retinopathy Study Research Group (ETDRS), "Photocoagulation for diabetic macular edema. ETDRS report no. 1," *Arch. Ophthalmol.* **103**(12), 1796–1806 (1985).
3. Early Treatment Diabetic Retinopathy Study Research Group, "Early photocoagulation for diabetic retinopathy. ETDRS report no. 9," *Ophthalmology* **98**(5 suppl), 766–785 (1991).
4. Branch Vein Occlusion Study Group, "Argon laser scatter photocoagulation for prevention of neovascularisation and vitreous hemorrhage in branch vein occlusion. A randomized clinical trial," *Arch. Ophthalmol.* **104**(1), 34–41 (1986).
5. The Central Vein Occlusion Study Group, "Natural history and clinical management of central retinal vein occlusion," *Arch. Ophthalmol.* **115**(4), 486–491 (1997).
6. A. Shah, N. Bressler, and L. Jampol, "Does laser still have a role in the management of retinal vascular and neovascular diseases?," *Am. J. Ophthalmol.* **152**(3), 332–339 (2011).
7. "Recommendation of the Retinological Society, the German Ophthalmological Society and the Professional Association of Ophthalmologists in Germany: treatment of diabetic maculopathy," *Klinische Monatsblätter Augenheilkunde* **228**(5), 446–459 (2011).
8. M. M. Muqit et al., "Spatial and spectral imaging of retinal laser photocoagulation burns," *Invest. Ophthalmol. Vis. Sci.* **52**(2), 994–1002 (2011).
9. Y. Nakamura et al., "Functional and morphological changes of macula after subthreshold micropulse diode laser photocoagulation for diabetic macular oedema," *Eye* **24**(5), 784–788 (2009).
10. M. M. Muqit et al., "Pain responses of Pascal 20 ms multi-spot and 100 ms single-spot panretinal photocoagulation: Manchester Pascal study, MAPASS report 2," *Br. J. Ophthalmol.* **94**(11), 1493–1498 (2010).
11. M. M. Muqit et al., "Single-session vs multiple-session pattern scanning laser panretinal photocoagulation in proliferative diabetic retinopathy: The Manchester Pascal study," *Arch. Ophthalmol.* **128**(5), 525–533 (2010).
12. M. Nagpal, S. Marlecha, and K. Nagpal, "Comparison of laser photocoagulation for diabetic retinopathy using 532-nm standard laser versus multispot pattern scan laser," *Retina* **30**(3), 452–458 (2010).
13. D. Lavinsky et al., "Randomized clinical trial evaluating mETDRS versus normal or high-density micropulse photocoagulation for diabetic macular edema," *Invest. Ophthalmol. Vis. Sci.* **52**(7), 4314–4323 (2011).
14. J. Roider et al., "Selective retina therapy (SRT) for clinically significant diabetic macular edema," *Graefes. Arch. Clin. Exp. Ophthalmol.* **248**(9), 1263–1272 (2010).
15. F. Bandello et al., "Light panretinal photocoagulation (LPRP) versus classic panretinal photocoagulation (CPRP) in proliferative diabetic retinopathy," *Semin. Ophthalmol.* **16**(1), 12–18 (2001).
16. Central Vein Occlusion Study Group, "Central vein occlusion study of photocoagulation therapy. Baseline findings," *Online J. Curr. Clin. Trials Doc.* **95** (1993).
17. M. S. Figueroa et al., "Laser photocoagulation for macular soft drusen," *Retina* **17**(5), 378–384 (1997).
18. A. Ho et al., "Laser-induced drusen reduction improves visual function at 1 year. Choroidal Neovascularization Prevention Trial Research Group," *Ophthalmology* **106**(7)1367–1373 (1999).
19. The Diabetic Retinopathy Study Research Group, "Photocoagulation treatment of proliferative diabetic retinopathy: the second report of diabetic retinopathy study findings," *Ophthalmology* **85**, 82–106 (1978).
20. The Diabetic Retinopathy Study Research Group, "Four risk factors for severe visual loss in diabetic retinopathy," *Arch. Ophthalmol.* **97**, 654–655 (1979).
21. R. Birngruber, V. P. Gabel, and F. Hillenkamp, "Experimental studies of laser thermal retinal injury," *Health Phys.* **44**(5), 519–531 (1983).
22. M. L. Wolbarsht and M. B. Landers, "The rationale of photocoagulation therapy for proliferative diabetic retinopathy: a review and a model," *Ophthalmic. Surg. Laser* **11**(4)235–245 (1980).
23. E. Boettner and J. R. Wolter, "Transmission of the ocular media," *Invest. Ophthalmol. Vis. Sci.* **1**, 776–783 (1962).
24. V. Gabel, R. Birngruber, and F. Hillenkamp, "Visible and near infrared light absorption in pigment epithelium and choroid," in *XIII Concilium Ophthalmologicum Kyoto*, N.-H. Elsevier, 658–662 (1978).
25. C. Sramek et al., "Dynamics of retinal photocoagulation and rupture," *J. Biomed. Opt.* **14**(3), 034007 (2009).
26. A. Jain et al., "Effect of pulse duration on size and character of the lesion in retinal photocoagulation," *Arch. Ophthalmol.* **126**(1), 78–85 (2008).
27. R. Birngruber, V. P. Gabel, and F. Hillenkamp, "Fundus reflectometry: a step towards optimization of the retina photocoagulation," *Mod. Probl. Ophthalmol.* **18**, 383–390 (1977).
28. Y. M. Paulus et al., "Healing of retinal photocoagulation lesions," *Invest. Ophthalmol. Vis. Sci.* **49**(12), 5540–5545 (2008).
29. R. Velez-Montoya et al., "Pattern scan laser photocoagulation: safety and complications, experience after 1301 consecutive cases," *Br. J. Ophthalmol.* **94**(6), 720–724 (2010).
30. V. Gabel, R. Birngruber, and B. Lorenz, "Clinical relevance of a dosing device for laser photocoagulation," *Klinische Monatsblätter Augenheilkunde* **188**, 263–265 (1986).
31. W. Weinberg et al., "Automatically dosed photocoagulation for the purpose of achieving reproducible effects in the fundus," *Fortschritte Ophthalmol.* **79**, 155–158 (1982).
32. R. Birngruber, F. Hillenkamp, and V. P. Gabel, "Theoretical investigations of laser thermal retinal injury," *Health Phys.* **48**(6), 781–796 (1985).
33. V. P. Gabel, R. Birngruber, and F. Hillenkamp, "Individuelle Unterschiede der Lichtabsorption am Augenhintergrund im sichtbaren und infraroten Spektralbereich," in *Ber. Dtsch Ophthalmol.*, G. W. Jaeger, Ed., J. F. Bergmann Verlag, München, Vol. **74**, pp. 418–421 (1977).
34. J. Kandulla et al., "Noninvasive optoacoustic online retinal temperature determination during continuous-wave laser irradiation," *J. Biomed. Opt.* **11**(4), 041111 (2006).
35. R. O. Esenaliev et al., "Real-time optoacoustic monitoring of temperature in tissues," *Proc. SPIE* **3601**, 268–275 (1999).
36. G. Schüle et al., "Optoacoustic measurements during μs-irradiation of the retinal pigment epithelium," *Proc. SPIE* **3914**, 230–236 (2000).
37. K. V. Larin, I. V. Larina, and R. O. Esenaliev, "Monitoring of tissue coagulation during thermotherapy using optoacoustic technique," *J. Phys. D: Appl. Phys.* **38**, 2645–2653 (2005).
38. I. V. Larina, K. V. Larin, and R. O. Esenaliev, "Real-time optoacoustic monitoring of temperatures in tissues," *J. Phys. D: Appl. Phys.* **38**, 2633–2639 (2005).
39. G. Schüle et al., "Non-invasive optoacoustic temperature determination at the fundus of the eye during laser irradiation," *J. Biomed. Opt.* **9**(1), 173–179 (2004).
40. M. L. Denton et al., "Spatially correlated microthermography maps threshold temperature in laser-induced damage," *J. Biomed. Opt.* **16**(3), 036003 (2011).
41. M. W. Sigrist, "Laser generation of acoustic waves in liquid and gases," *J. Appl. Phys.* **60**, 85–121 (1986).
42. G. Paltauf and P. E. Dyer, "Photomechanical processes and effects in ablation," *Chem. Rev.* **103**(2), 487–518 (2003).
43. G. Paltauf and H. Schmidt-Kloiber, "Microcavity dynamics during laser-induced spallation of liquids and gels," *Appl. Phys. A: Mater. Sci. Process* **62**, 303–311 (1996).

44. M. Hammer et al., "Optical properties of ocular fundus tissues - an in vitro study using the double-integrating-sphere technique and inverse Monte Carlo simulation," *Phys. Med. Biol.* **40**(6), 963–978, (1995).
45. A. Vassiliadis, "Ocular damage from laser radiation" in *Laser Applications in Medicine and Biology*, Plenum Publishing Corporation, New York (1971).
46. K. Schlott et al., "Automatic temperature controlled retinal photocoagulation," *J. Biomed. Opt.*, scheduled for publication (June 2012).
47. A. Baade et al., "Accuracy of real-time optoacoustic temperature determination during retinal photocoagulation," *Proc. SPIE* **8092**, 80921B (2011).
48. R. Brinkmann et al., "Realtime temperature determination during retinal photocoagulation on patients," *Proc. SPIE* **7885**, 78850R (2011).
49. H. Müller et al., "Imaging thermal expansion and retinal tissue changes during photocoagulation by high speed OCT," *Biomed. Opt. Express* **35**(5), 1025–1046 (2012).
50. K. Schlott et al., "Time resolved detection of tissue denaturation during retinal photocoagulation," *Proc. SPIE* **7373**, 73730E (2009).
51. K. Schlott et al., "Optoacoustic temperature determination and automatic coagulation control in rabbits," *Proc. SPIE* **7885**, 78850T (2011).
52. S. Koinzer et al., "Temperature controlled retinal photocoagulation - a step toward automated laser treatment," *IOVS* (2012) (accepted for publication).